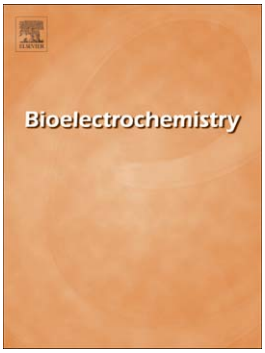

Electrochemically driven biocatalysis of the oxygenase domain of neuronal nitric oxide synthase in indium tin oxide nanoparticles/polyvinyl alcohol nanocomposite

Xuan Xu, Jing Qian, Songqin Liu

PII: S1567-5394(13)00051-0
DOI: doi: 10.1016/j.bioelechem.2013.04.005
Reference: BIOJEC 6676

To appear in: *Bioelectrochemistry*

Received date: 6 December 2012
Revised date: 2 April 2013
Accepted date: 23 April 2013

Please cite this article as: Xuan Xu, Jing Qian, Songqin Liu, Electrochemically driven biocatalysis of the oxygenase domain of neuronal nitric oxide synthase in indium tin oxide nanoparticles/polyvinyl alcohol nanocomposite, *Bioelectrochemistry* (2013), doi: 10.1016/j.bioelechem.2013.04.005

Electrochemically driven biocatalysis of the oxygenase domain of neuronal nitric oxide synthase in indium tin oxide nanoparticles/polyvinyl alcohol nanocomposite

Xuan Xu, Jing Qian, Songqin Liu*
School of Chemistry and Chemical Engineering, Southeast University, Nanjing, 211189, P. R. China
* Corresponding author. Tel: +86-25-52090613. Fax: +86-25-52090618. E-mail:liusq@seu.edu.cn.

ABSTRACT

Nitric oxide synthase (NOS) plays a critical role in a number of key physiological and pathological processes. Investigation of electron-transfer reactions in NOS would contribute to a better understanding of the nitric oxide (NO) synthesis mechanism. Herein, we describe an electrochemically driven catalytic strategy, using a nanocomposite consisted of the oxygenase domain of neuronal NOS (D290nNOSoxy), indium tin oxide (ITO) nanoparticles and polyvinyl alcohol (PVA). Fast direct electron transfer between electrodes and D290nNOSoxy was observed with the heterogeneous electron transfer rate constant (k_{et}) of 154.8±0.1 s^{-1} at the scan rate of 5 Vs^{-1}. Moreover, the substrate N^{ω}-hydroxy-L-arginine (NHA) was used to prove the concept of electrochemically driven biocatalysis of D290nNOSoxy. In the presence of the oxygen cosubstrate and tetrahydrobiopterin (BH4) cofactor, the addition of NHA caused the decreases of both oxidation current at +0.1 V and reduction current at potentials ranging from -0.149 V to -0.549 V *vs* Ag/AgCl. Thereafter, a series of control experiments such as in the absence of BH4 or D290nNOSoxy were performed. All the results demonstrated that D290nNOSoxy biocatalysis was successfully driven by electrodes in the presence of BH4 and oxygen. This novel bioelectronic system showed potential for further investigation of NOS and biosensor applications.

Keywords:
Nitric oxide synthase, Tetrahydrobiopterin, N^{ω}-hydroxy-L-arginine, Indium tin oxide nanoparticles, Biocatalysis

1. Introduction

Nitric oxide (NO) is one of the ubiquitous cellular signaling molecule involving an amazing range of physiologic effects, including neurotransmission, vasodilation, cytotoxicity, and involvement in almost all pathologic states [1-3]. In mammalian species, NO is synthesized by nitric oxide synthase (NOS), a homodimeric flavo-hemoprotein that catalyzes the five-electron oxidation of L-arginine (L-Arg) to NO and L-citrulline (Cit) via two steps with an intermediate of N^{ω}-hydroxy-L-arginine (NHA) [4]. Heme iron is involved in both steps of the NOS reactions [5], and the overall reaction is similar to the monooxygenations catalyzed by cytochrome P450 [6,7].

Three isoforms of NOS enzymes have been characterized: neuronal NOS (nNOS), inducible NOS (iNOS), and endothelial NOS (eNOS). Though different in size, amino acid, sequence, expression level and functions of the evolved NO product, these isoforms display a lot of structural and mechanism similarities. Each NOS enzyme consists of two domains, an N-terminal oxygenase domain and a C-terminal reductase domain. The former contains a cysteine-ligated heme and binding sites for the tetrahydrobiopterin (BH4) cofactor and the substrates of L-Arg or NHA [8,9], while the latter has binding sites for NADPH, flavin adenine dinucleoide (FAD) and flavin mononucleotide (FMN). As revealed in previous studies, these two domains are linked by a polypeptide chain as a binding site for calmodulin (CaM) [10,11]. The FAD and FMN prosthetic groups transfer electrons from NADPH to the heme iron. And, CaM-binding activates the interdomain electron transfer reaction in eNOS and nNOS [12].

The role of BH4 cofactor in NOS catalysis has been extensively studied. Specifically, BH4-binding to NOS influences enzyme dimerization [13], binding affinity for substrates [14], heme midpoint potential [15] and stability of heme-dioxy complex [16]. However, the function of BH4 cofactor in NOS catalysis can not be completely explained by these effects. A variety of studies suggested that the redox properties of BH4 are essential to its functions in NOS catalysis. It was speculated that BH4 might provide the second electron to a heme-dioxy complex for oxygen activation, during which a BH4 radical (BH3·) was formed as illustrated in Scheme 1 [17,18,19]. Further evidence indicates that the generated radical BH3· in the first step of L-Arg hydroxylation must be reduced back to BH4 before the second step of NO synthesis starts [20,21]. Besides, it is noted that the one-electron-transfer role of BH4 is unique to NOS, which is fundamentally different from other enzymes that utilize BH4 as a substrate or cofactor [8, 22-24].

Here Scheme 1

Using the purified heme oxygenase domain of nNOS, the direct electron exchange between electrodes and the enzyme in didodecyldimethylammonium bromide film has been investigated [6]. In the same film, the direct electrochemistry of iNOS on the surface of basal plane graphite electrodes was has also been achieved. Based on the pH-dependent data, the heme axial water ligand gates electron transfer in iNOS was demonstrated [7]. However, there remains an unmet challenge to drive the catalytic cycle in the way of delivering electrons from electrodes to enzyme so as to replace the electron donation of co-enzyme such as NADPH [6,7]. The electrochemically driven strategy would promote the development of inexpensive and rapid assays or biosensors, which would not only enable electrochemical investigation of the catalytic

pathway but also simplify the applications for biological synthesis [25-27].

In this paper, the oxygenase domain of nNOS (D290nNOSoxy) was embedded into a nanocomposite which combined the good conductivity of indium tin oxide (ITO) nanoparticles with the remarkable biocompatibility of polyvinyl alcohol (PVA), and the direct electron transfer between D290nNOSoxy and electrodes was investigated. Moreover, the catalytic behavior of D290nNOSoxy was studied, during which the electrode was used as the electron source instead of NADPH. Furthermore, the critical functions of BH4 and oxygen in nNOS biocatalysis process were verified by a series of control experiments.

2. Experimental section

2.1. Reagents

The oxygenase domain of neuronal nitric oxide synthase without residues 1-290 (D290nNOSoxy) was expressed and purified as described earlier [28]. The molecular weight (MW) of D290nNOSoxy was about 49 kDa. Polyvinyl alcohol (PVA, MW 22000) was purchased from Serva. Indium tin oxide (ITO, nanoparticles with an average diameter of ca. 10-40 nm, dispersion, 25 wt% in isopropanol,) and tetrahydrobiopterin (BH4) were obtained from Sigma-Aldrich Chem. Co. N^{ω}-hydroxy-L-arginine (NHA) was purchased from Calbiochem. Phosphate buffer solution (PBS, 0.1 M, pH 7.0) was prepared by mixing the stock solution of K_2HPO_4 and KH_2PO_4. Deionized water was prepared with a Millipore system. Other reagents were of analytical reagent grade unless otherwise specified and were used as received.

2.2. Electrode preparation

The glassy carbon electrode (GCE) with a diameter of 3 mm was successively polished using 1.0 and 0.3 μm alumina powder, followed by rinsing thoroughly with deionized water. After successive sonication in 1:1 nitric acid, acetone and deionized water, the electrode was rinsed with deionized water and dried at room temperature.

To prepare D290nNOSoxy modified electrode, 1.42 μL of PVA (170 μg/mL), 5.38 μL of H_2O, 1.2 μL of ITO nanoparticles (25 wt% in isopropanol) and 4 μL of D290nNOSoxy were mixed together. Then 10 μL of this mixture was dropped on the surface of the pretreated GCE to obtain D290nNOSoxy/ITO/PVA/GCE. For control experiments, only 10 μL of the mixture of H_2O, ITO nanoparticles and PVA was casted onto the surface of GCE to obtain ITO/PVA/GCE. All modified electrodes were dried at 4 ^{o}C overnight to allow the formation of uniform films and were thoroughly rinsed with deionized water before use.

2.3. Apparatus and procedures

Cyclic voltammetry (CV) and square wave voltammetry (SWV) were performed on a computer-controlled electrochemical analyzer (CHI440, CHI Instrument) with the conventional three-electrode system composed of modified GCE as the working electrode, platinum wire as the counter electrode and a KCl saturated Ag/AgCl as the reference electrode. To create the anaerobic environment, the buffer solution was bubbled thoroughly with high-purity nitrogen for 10 min before use. All experiments were carried out at the ambient temperature of about 25 °C.

The morphology of ITO/PVA nanocomposite was characterized by using scanning

electron microscopy (SEM, JEOLJSM-5610LV, Japan) and transmission electron microscopy (TEM, JEOL JEM-100S, Japan).

3. Results and discussion

3.1. Electrochemical behaviors of D290nNOSoxy entrapped in ITO/PVA nanocomposite

PVA was well-known for its excellent film-forming ability, high solvent permeability, good adhesion, and remarkable biocompatibility [29,30]. ITO nanoparticles have advantages of its high electrical conductivity over a broad potential window which facilitates electron transport toward the electroactive centers of proteins [31,32]. The microstructure of ITO/PVA nanocomposite was investigated by SEM and TEM. The SEM image in Fig. 1A shows that ITO nanoparticles were dispersed well in PVA and a uniform film was formed on the electrode surface. From the TEM image (Fig. 1B), it is seen that the film was extremely porous, providing a suitable microenvironment to keep the bioactivity of D290nNOSoxy.

Here Fig. 1

The electron transfer properties of D290nNOSoxy in ITO/PVA nanocomposite were investigated by the electrochemical measurements. As shown in Fig. 2A, the CV curve of D290nNOSoxy/ITO/PVA/GCE gave a pair of well-defined redox peaks in oxygen-free solution at the scan rate of 9 Vs^{-1}, while no peaks were observed on ITO/PVA/GCE in the same potential window. Obviously, the redox peaks corresponded to the heme iron (Fe^{II}/Fe^{III}) redox couple in D290nNOSoxy. The formal potential of -0.385 V *vs* Ag/AgCl was consistent with other studies of heme proteins [32,33].

Here Fig. 2

At lower scan rates from 0.01 to 0.5 Vs^{-1}, the reduction peak was pronounced while the oxidation peak was very small, which was probably due to the interference of residual oxygen in the film and solution [34]. At higher scan rates ranging from 3 to 19 Vs^{-1}, the reduction and oxidation peak currents rose linearly with the linear equations as $I_{pc}(\mu A) = (0.871\pm0.036)\ \nu(Vs^{-1}) + (3.404\pm0.434)$ (R=0.995) and $I_{pa}(\mu A) = (-0.431\pm0.009)\ \nu(Vs^{-1}) - (0.051\pm0.115)$ (R=0.996), respectively (inset in Fig. 2A), suggesting a surface-controlled process. The small peak-to-peak separation of 42±1 mV at the scan rate of 5 Vs^{-1} indicated the fast electron transfer rate between electrodes and the redox protein in the immobilized layer. The heterogeneous transfer rate constant of the first electron (k_{et}) was estimated to be 154.8±0.1 s^{-1} at the scan rate of 5 Vs^{-1} by the method of Laviron [35]. The value was comparable with former studies of 80.0 s^{-1} at 10 Vs^{-1} for cytochrome P450 2B4 on modified electrodes with nonionic detergent and colloidal clay nanoparticles [34], 350.0 s^{-1} at 16.7 Vs^{-1} for iNOS in DDAB films on the surface of BPG electrodes [7], and 12.3 s^{-1} at 0.5 Vs^{-1} for cytochrome P450 2C9 in CYP2C9/CRP-microsome/ITO/CS [32]. These investigations clearly suggested that the film of ITO/PVA nanocomposite provided a favorable bioenvironment for the immobilization of proteins exposing redox active site in the event of electron-transfer.

Electron transfer in biological systems is often accompanied with proton movement. The variation of the reduction potentials with pH was plotted in Fig. 2B. The increase

of pH from 5.5 to 8.5 caused a negative shift of the formal potential with the linear equation as E(V) = (-0.047±0.001) pH + (0.044±0.012) (R=0.991). The slope of -47±1 mV/pH unit was close to the value found for a reduction process involving one electron and one proton [36]. Actually, the distal pocket of heme was hydrophobic and hence lacked obvious proton-donating residues when the hydrophilic substrate was absent. The proton-coupled electron transfer demonstrated that the structure of NOS might control the electron transfer to the heme active site in another yet unknown process [7, 37].

3.2. Electrochemistry of free BH4

In spite of some differences between the redox properties of enzyme-bound BH4 and free BH4, the electrochemical behavior of free BH4 is still appealing. Fig. 3A shows CV curves obtained on bare GCE in anaerobic solution with different concentrations of BH4. As the concentration of BH4 increased, the peak current at +0.1 V *vs* Ag/AgCl increased obviously. To further characterize the oxidation reaction at +0.1 V, CVs were performed at different scan rates (data not shown). As the scan rates varied from 0.1 to 0.5 Vs^{-1}, the peak current at +0.1 V increased proportionally with the square root of the scan rates and the relationship was shown as $I_p(\mu A) = (-0.063\pm0.009)\ v^{1/2}(mVs^{-1})^{1/2} - (0.094\pm0.001)$ (R=0.998). Besides, the difference between potentials of the maximal and half-maximal currents $|E_P-E_{P/2}|$ was 55.4 mV, which suggested that it was an electrochemically reversible one-electron oxidation reaction at +0.1 V [22]. Actually, the one-electron oxidation product of BH4 is the radical BH3· that has been observed in catalytic reactions with the heme domain of nNOS [38] and iNOS [8].

Here Fig. 3

However, as the radical BH3· was extremely thermodynamically unstable, it would remove the second electron rapidly and form the two-electron oxidation product of quinonoid BH2 (qBH2), which would be reduced at -0.4 V *vs* Ag/AgCl [22, 39]. As a result, the more BH4 was oxidized at +0.1 V, the more qBH2 was generated, giving rise to the reduction current at -0.4 V (Fig. 3A). Generally, unstable qBH2 was rearranged to form 7,8-dihydrobiopterin (7,8-BH2), which would be oxidized at the higher potential [40]. Under this experimental condition, there was a small oxidation peak of 7,8-BH2 at +0.7 V *vs* Ag/AgCl. Owing to the short scan time, only a small amount of 7,8-BH2 was generated from qBH2 [22, 39].

In aerobic solution, several factors including pH, temperature and buffer can influence the oxidation behavior of BH4 [41]. Fig. 3B shows the CV curves of the freshly prepared BH4 before and after being kept in aerobic PBS (0.1 M, pH 7.0) for 12 h. After aerobic oxidation, the two peaks at +0.1 V and -0.4 V disappeared completely, while a sharp oxidation peak appeared at +0.7 V *vs* Ag/AgCl which was ascribed to the oxidation of 7,8-BH2. At the same time, the small peak emerging at +0.5 V indicated the generation of another unknown auto-oxidation product of BH4. However, no obvious change in CV curves was observed after aerobic oxidation for 2 h in the same solution (data not shown). These results evidently indicated that BH4 was able to be oxidized slowly in aerobic 0.1 M pH 7.0 PBS and the predominant oxidation product was 7,8-BH2 [42,43]. To maintain the activity of BH4, all the BH4 solution used in the following experiments was freshly prepared.

3.3. Electrochemically driven biocatalysis

After the addition of BH4 and incubation for 10 min, the reduction potential of D290nNOSoxy heme moved from -0.243 V to -0.271 V *vs* Ag/AgCl (Fig. 4). The similar behavior has been observed for nNOS oxygen domain by spectroelectrochemical titrations [15].

Here Fig. 4

The negative shift of the reduction potential of D290nNOSoxy implied that BH4 had a lower affinity to the reduced form of D290nNOSoxy compared with its affinity to the oxidized form [15,27]. The following equation illustrated the relationship between the binding constants of BH4 to the reduced form of enzyme ($K_{D,red}$) and to the oxidized form of enzyme ($K_{D,ox}$).

$$K_{D,red}=10^{-[(Em,b\ -Em,f)\ nF/\ (2.303RT)]}K_{D,ox} \qquad (1)$$

where Em,b is the measured reduction potential of BH4-bound enzyme, Em,f is the measured reduction potential of BH4-free enzyme, R is the gas constant, F is the Faraday constant, and T is the experimental temperature [15]. According to eq. 1, the quantitative relationship between $K_{D,red}$ and $K_{D,ox}$ was illustrated as $K_{D,red}$ = (2.98±0.01) $K_{D,ox}$ (for one-electron reaction at 25 °C), which meant that the binding affinity of BH4 to the ferrous heme form of D290nNOSoxy decreased by about 3-fold of that to the oxidized form. This result was consistent with the electron donating role of BH4 to the ferrous-dioxygen complex of nNOS [17-19] and the BH4 binding site in close proximity to the heme center [8,9]. As a result, when the heme was reduced, it was difficult for BH4 to get bound to the active site of nNOS. Besides, upon BH4 binding, the heme center would become hard to be reduced by the electrode.

In the presence of oxygen, the same electrochemical experiment was carried out on D290nNOSoxy/ITO/PVA/GCE. As shown in Fig. 5A, the introduction of oxygen dramatically changed the shape of CV curves for D290nNOSoxy heme, together with an increased reduction current and a decreased oxidation current, suggesting a typical electrocatalytic oxygen reduction process and the fast binding of oxygen to the ferrous heme [6,32,44]. After the addition of BH4 cofactor and incubation for 10 min, the reduction potential of D290nNOSoxy negatively shifted from -0.258 V to -0.286 V *vs* Ag/AgCl, which was similar to that observed in oxygen-free solution, implying the successful binding of BH4 to the active site of D290nNOSoxy. Interestingly, BH4-binding to D290nNOSoxy under the aerobic condition made the reduction current of D290nNOSoxy increase obviously (Fig. 5A, curve c), whereas it decreased with the addition of BH4 in the anaerobic atmosphere (Fig. 4, curve b). The discrepancy might indicate that the bound BH4 had provided electrons for the ferrous-dioxygen complex and sped the oxygen activation of the ferrous heme domain [16,17,19].

Here Fig. 5

NHA, the substrate which can be directly catalyzed by nNOS to yield NO [4,5], was used to prove the concept of electrochemically driven catalysis of D290nNOSoxy. When the BH4 cofactor and oxygen cosubstrate were present, the addition of NHA caused decreases of both the oxidation current at +0.1 V and the reduction current

ranging from -0.149 V to -0.549 V (Fig. 5A, curve d). In the control experiments, no change was observed on ITO/PVA/GCE or when the same volume of PBS was added into the solution (data not shown). The above findings might indicate the occurrence of the electrochemically driven catalysis of D290nNOSoxy. As NO synthesis was an oxygen-dependent process [4], the decreased reduction current could be due to the consumption of oxygen in the catalysis process.

To further verify the critical function of BH4 in nNOS biocatalysis, NHA was added into aerobic PBS in the absence of BH4. As shown in Fig. 5B, the addition of NHA made the reduction potential of D290nNOSoxy heme positively shift from -0.318 V to -0.282 V, but the reduction current changed little. The positive movement of the heme reduction potential has been proved to be correlated to the low-to-high spin shift of nNOS upon substrate binding, which acted as a gate of the NOS catalytic cycle by facilitating the first electron transfer [6,21]. Meanwhile, the lack of decreased reduction current suggested that the amount of oxygen in the solution was not consumed after the addition of NHA. In other words, the electrochemically driven catalysis of D290nNOSoxy hardly occurred without BH4. Therefore, it was reasonable to predict that the above decreased oxidation current at +0.1 V (Fig. 5A, curve d) was caused by the depletion of BH4, which would be converted into radicals when it participated in NO synthesis.

All the measurements were repeated for three times with the same modified electrode and the same result was obtained. Therefore, we infer that the electrochemically biocatalysis of D290nNOSoxy was successfully driven by electrodes, and the oxygen cosubstrate and BH4 cofactor played significant roles in the catalysis process.

4. Conclusions

In summary, an electrochemically driven biocatalysis of D290nNOSoxy was successfully constructed by integrating D290nNOSoxy, ITO nanoparticles and PVA. The nanocomposite provided a favorable bioenvironment for maintaining the bioactivity of immobilized enzymes, making it an idea platform for the studies of NOS catalysis process. This novel bioelectronic system had potential for further research of NO synthesis mechanism and bioreactor/biosensor applications. We were also pursuing studies to understand the regulation of L-Arg conversion driven by D290nNOSoxy/ITO/PVA/GCE, and how BH4 affected this biocatalysis process.

Acknowledgement

We gratefully acknowledge the Key Program (21035002) from the National Natural Science Foundation of China, the National Basic Research Program of China (No.2010CB732400), National Natural Science Foundation of China (Grant Nos. 21175021), Foundation for Excellent Doctoral Dissertation from Southeast University (YBJJ1112) and Scholarship Award for Excellent Doctoral Student granted by Ministry of Education. We also thank Prof. Dr. Ulla Wollenberger for her helpful discussions and the provision of D290nNOSoxy.

References

[1] H. H. W. S. Harald, U. Walter, NO at work, Cell 78 (1994) 919-925.
[2] E. Culotta, D. E. Koshland, NO news is good news, Science 258 (1992) 1862-1865.
[3] S. Moncada, E. A. Higgs, The discovery of nitric oxide and its role in vascular biology, Br. J. Pharmacol. 147 (2006) S193–S201.
[4] W. K. Alderton, C. E. Cooper, R. G. Knowles, Nitric oxide synthases: structure, function and inhibition, Biochem. J. 357 (2001) 593-615.
[5] K. A. White, M. A. Marletta, Nitric oxide synthase is a cytochrome P-450 type hemoprotein, Biochemistry 31 (1992) 6627-6631.
[6] M. Bayachou, J. A. Boutros, Direct electron transfer to the oxygenase domain of neuronal nitric oxide synthase (NOS): exploring unique redox properties of NOS enzymes, J. Am. Chem. Soc. 126 (2004) 12722-12723.
[7] A. K. Udit, W. Belliston-Bittner, E. C. Glazer, Y. H. L. Nguyen, J. M. Gillan, M. G. Hill, M. A. Marletta, D. B. Goodin, H.B. Gray, Redox couples of inducible nitric oxide synthase, J. Am. Chem. Soc. 127 (2005) 11212-11213.
[8] J. Zhang, P. Martasek, R. Paschke, T. Shea, B. S. S. Masters, J. P. Kim, Crystal structure of the FAD/NADPH-binding domain of rat neuronal nitric-oxide synthase, J. Biol. Chem. 276 (2001) 37506-37513.
[9] C. S. Raman, H. Li, P. Martasek, V. Kral, Bettie S. S. Masters, T. L. Poulos, Crystal structure of constitutive endothelial nitric oxide synthase: a paradigm for pterin function involving a novel metal center, Cell 95 (1998) 939-950.
[10] J. Yadav, I. Sagami, T. Shimizu, Cyanide binding study of neuronal nitric oxide synthase: effects of inhibitors and mutations at the substrate binding site, J. Inorg. Biochem. 95 (2003) 25–30.
[11] D. S. Bredt, P. M. Hwang, C. E. Glatt, C. Lowenstein, R. R. Reed, S. H. Snyder, Cloned and expressed nitric oxide synthase structurally resembles cytochrome P-450 reductase, Nature 351 (1991) 714-718.
[12] C. Feng, G. Tollin, Regulation of interdomain electron transfer in the NOS output state for NO production, Dalton Trans. 34 (2009) 6692–6700.
[13] H. M. Abu-Soud, M. Loftus, D. J. Stuehr, Subunit dissociation and unfolding of macrophage NO synthase: relationship between enzyme structure, prosthetic group binding, and catalytic function, Biochemistry 34 (1995) 11167-11175.
[14] B. Mayer, C. Wu, A. C. F. Gorren, S. Pfeiffer, K. Schmidt, P. Clark, D. J. Stuehr, E. R. Werner, Tetrahydrobiopterin binding to macrophage inducible nitric oxide synthase: heme spin shift and dimer stabilization by the potent pterin antagonist 4-amino-tetrahydrobiopterin, Biochemistry 36 (1997) 8422-84227.
[15] A. Presta, A. M. Weber-Main, M. T. Stankovich, D. J. Stuehr, Comparative effects of substrates and pterin cofactor on the heme midpoint potential in inducible and neuronal nitric oxide synthases, J. Am. Chem. Soc. 120 (1998) 9460-9465.
[16] H. M. Abu-Soud, R. Gachhui, F. M. Raushe, D. J. Stuehr, The ferrous-dioxy complex of neuronal nitric oxide synthase, J. Biol. Chem. 272 (1997) 17349-53.
[17] A. R. Hurshman, C. Krebs, D. E. Edmondson, M. A. Marletta, Ability of tetrahydrobiopterin analogues to support catalysis by inducible nitric oxide synthase: formation of a pterin radical is required for enzyme activity, Biochemistry 42 (2003) 13287-13303.
[18] A. R. Hurshman, C. Krebs, D. E. Edmondson, B. H. Huynh, M. A. Marletta, Formation of a pterin radical in the reaction of the heme domain of inducible nitric oxide synthase with oxygen, Biochemistry 38 (1999) 15689-15696.

[19] C. C. Wei, B. R. Crane, D. J. Stuehr, Tetrahydrobiopterin radical enzymology, Chem. Rev. 103 (2003) 2365−2383.
[20] A. C. F. Gorren, N. Bec, A. Schrammel, E. R. Werner, R. Lange, B. Mayer, Low-temperature optical absorption spectra suggest a redox role for tetrahydrobiopterin in both steps of nitric oxide synthase catalysis, Biochemistry 39 (2000) 11763-11770.
[21] A. R. Hurshman, M.A. Marletta, Reactions catalyzed by the heme domain of inducible nitric oxide synthase: evidence for the involvement of tetrahydrobiopterin in electron transfer, Biochemistry 41 (2002) 3439-3456.
[22] A. C. F. Gorren, A. J. Kung, K. Schmidt, E. R. Werner, B. Mayer, Electrochemistry of pterin cofactors and inhibitors of nitric oxide synthase, Nitric Oxide 5 (2001) 176-186.
[23] S. Stoll, Y. NejatyJahromy, J. J. Woodward, A. Ozarowski, M. A. Marletta, R. D. Britt, Nitric oxide synthase stabilizes the tetrahydrobiopterin cofactor radical by controlling its protonation state, J. Am. Chem. Soc. 132 (2010) 11812-11823.
[24] Z. Wang, C. Wei, S. Ghosh, A. L. Meade, C. Hemann, R. Hille, D. J. Stuehr, A conserved tryptophan in nitric oxide synthase regulates heme-dioxy reduction by tetrahydrobiopterin, Biochemistry 40 (2001) 12819-12825.
[25] S. Krishnan, D. Wasalathanthri, L. Zhao, J. B. Schenkman, J. F. Rusling, Efficient bioelectronic actuation of the natural catalytic pathway of human metabolic cytochrome P450s, J. Am. Chem. Soc. 133 (2011) 1459-1465.
[26] A. Fantuzzi, M. Fairhead, G.. Gilardi, Direct electrochemistry of immobilized human cytochrome P450 2E1, J. Am. Chem. Soc. 126 (2004) 5040-5041.
[27] A. Shukla, E. M. Gillam, D. J. Mitchell, P. V. Bernhardt, Direct electrochemistry of enzymes from the cytochrome P450 2C family, Electrochem. Commun. 7 (2005) 437-442.
[28] C. Jung, F. Lendzian, V. Schunemann, M. Richter, L. H. Bottger, A. X. Trautwein, J. Contzen, M. Galander, D. K. Ghosh, A. Barra, Multi-frequency EPR and mossbauer spectroscopic studies on freeze-quenched reaction intermediates of nitric oxide synthase, Magn. Reson. Chem. 43 (2005) S84-S95.
[29] M. I. Baker, S. P. Walsh, Z. Schwartz, B. D. Boyan, A review of polyvinyl alcohol and its uses in cartilage and orthopedic applications. J. Biomed. Mater. Res. Part B 100B (2012) 1451–1457.
[30] Y. Fang, D. Zhang, X. Qin, Z. Miao, S. Takahashi, J. Anzai, Q. Chen, A non-enzymatic hydrogen peroxide sensor based on poly(vinyl alcohol)–multiwalled carbon nanotubes–platinum nanoparticles hybrids modified glassy carbon electrode, Electrochim. Acta 70 (2012) 266–271.
[31] Y. Aksu, S. Frasca, U. Wollenberger, M. Driess, A. Thomas, A molecular precursor approach to tunable porous tin-rich indium tin oxide with durable high electrical conductivity for bioelectronic devices, Chem. Mater. 23 (2011) 1798–1804.
[32] X. Xu, W. Wei, M. H. Huang, L. Yao and S. Q. Liu, Electrochemically driven drug metabolism via cytochrome P450 2C9 isozyme microsomes with cytochrome P450 reductase and indium tin oxide nanoparticle composites, Chem. Commun. 48 (2012) 7802–7804.
[33] G. Shi, Z. Sun, M. Liu, L. Zhang, Y. Liu, Y. Qu, L. Jin, Electrochemistry and electrocatalytic properties of hemoglobin in layer-by-layer films of SiO_2 with vapor-surface sol-gel deposition, Anal. Chem. 79 (2007) 3581-3588.
[34] V. V. Shumyantseva, Y. D. Ivanov, N. Bistolas, F. W. Scheller, A. I. Archakov, U. Wollenberger, Direct electron transfer of cytochrome P450 2B4 at electrodes modified with nonionic detergent and colloidal clay nanoparticles, Anal. Chem. 76 (2004)

6046-6052.
[35] E. Labiron, General expression of the liner potential sweep voltammogram in the case of diffusion electrochemical systems, J. Electroanal. Chem. 101 (1979) 19-28.
[36] A. M. Bond, Modern Polarographic Methods in Analytical Chemistry, Marcel Dekker, New York, 1980.
[37] B. R. Crane, A. S. Arvai, D. K. Ghosh, C. Q. Wu, E. D. Getzoff, D. J. Stuehr, J. A. Tainer, Structure of nitric oxide synthase oxygenase dimer with pterin and substrate, Science 279 (1998) 2121-2126.
[38] N. Bec, A. F. C. Gorren, B. Mayer, P. P. Schmidt, K. K. Andersson, R. Lange, The role of tetrahydrobiopterin in the activation of oxygen by nitric-oxide synthase, J. Inorg. Biochem. 81 (2000) 207-211.
[39] K. R. Hoke, B. R. Crane, The solution electrochemistry of tetrahydrobiopterin revisited, Nitric Oxide 20 (2009) 79–87.
[40] R. Raghavan, G. Dryhurst, Redox chemistry of reduced pterin species, J. Electroanal. Chem. Interfac. Electrochem. 129 (1981) 189–212.
[41] J. A. Blair, A. J. Pearson, Some observations on the effects of light and solvent polarity on the kinetics of tetrahydrobiopterin autoxidation, J. Chem. Soc. 2 (1974) 1786-1787.
[42] M. D. Davis, S. Kaufman, S. Milstien, The auto-oxidation of tetrahydrobiopterin, Eur. J. Biochem. 173 (1988) 345-3521.
[43] S. Kaufman, Metabolism of the phenylalanine hydroxylation cofactor, J. Biol. Chem. 242 (1967) 3934-3943.
[44] S. Q. Liu, L. Peng, X. D. Yang, Y. F. Wu, L. He, Electrochemistry of cytochrome P450 enzyme on nanoparticle-containing membrane-coated electrode and its applications for drug sensing, Anal. Biochem. 375 (2008) 209-216.

Captions

Scheme 1. Oxidation reaction of L-Arg and NHA by NOS.

Fig. 1. (A) SEM and (B) TEM images of ITO/PVA nanocomposite.

Fig. 2. (A) CV curves obtained on (a) D290nNOSoxy/ITO/PVA/GCE and (b) ITO/PVA/GCE at the scan rate of 9 Vs^{-1} in anaerobic 0.1 M pH 7.0 PBS. The inset shows dependence of peak currents on scan rates. (B) SWV with 50 mV amplitude and 10 Hz frequency on D290nNOSoxy/ITO/PVA/GCE in anaerobic 0.1 M PBS with different pH of 5.5, 6, 6.5, 7, 7.5, 8, 8.5 (from down to up). The inset is the linear relationship between pH and the formal potential of the reduction peak of D290nNOSoxy.

Fig. 3. (A) CV curves obtained on bare GCE in anaerobic 0.1 M pH 7.0 PBS with (a) 52.83 μM, (b) 101.54 μM and (c) 149.52 μM BH4. (B) CV curves in 149.52 μM BH4 (a) before and (b) after being kept in aerobic 0.1 M pH 7.0 PBS for 12 h. Scan rate: 0.5 Vs^{-1}.

Fig. 4. CV curves obtained on D290nNOSoxy/ITO/PVA/GCE (a) without and (b) with the addition of 52.83 μM BH4 and incubation for 10 min. Electrolyte: anaerobic 0.1 M pH 7.0 PBS, scan rate: 1 mVs^{-1}.

Fig. 5. (A) CV curves obtained in 0.1 M pH 7.0 PBS that was (a) nitrogen saturated, (b) air saturated, (c) air saturated with the addition of 40 μM BH4 and incubation for 10 min, and (d) with the continued addition of 731 μM NHA. (B) CV curves obtained on D290nNOSoxy/ITO/PVA/GCE in BH4-free solution (a) before and (b) after the addition of 366 μM NHA. Scan rate: 1 mVs^{-1}.

Scheme 1

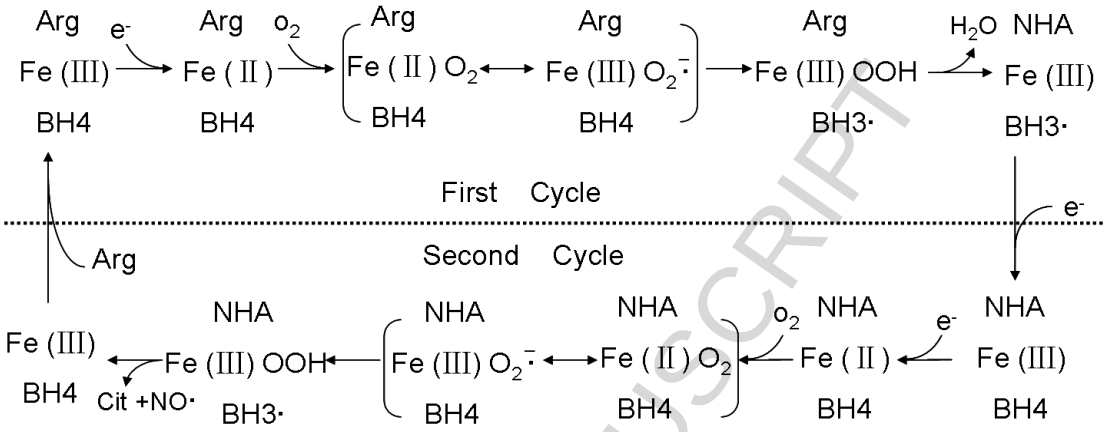

Fig. 1

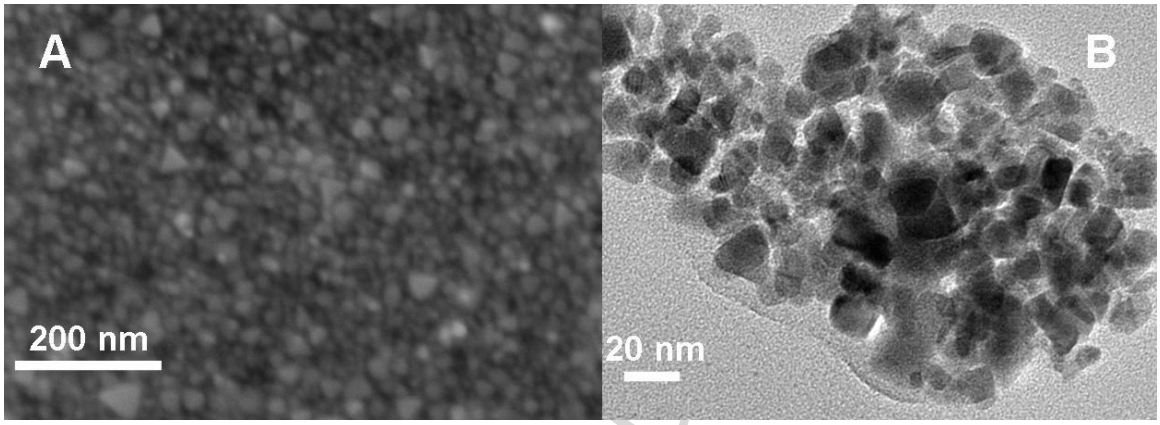

Fig. 2

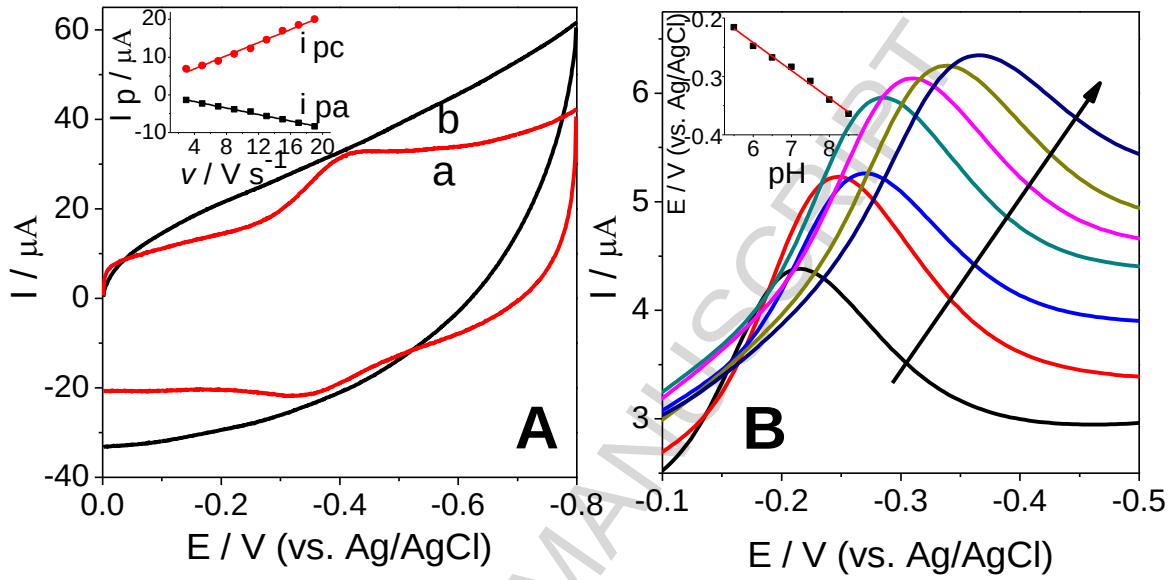

Fig. 3

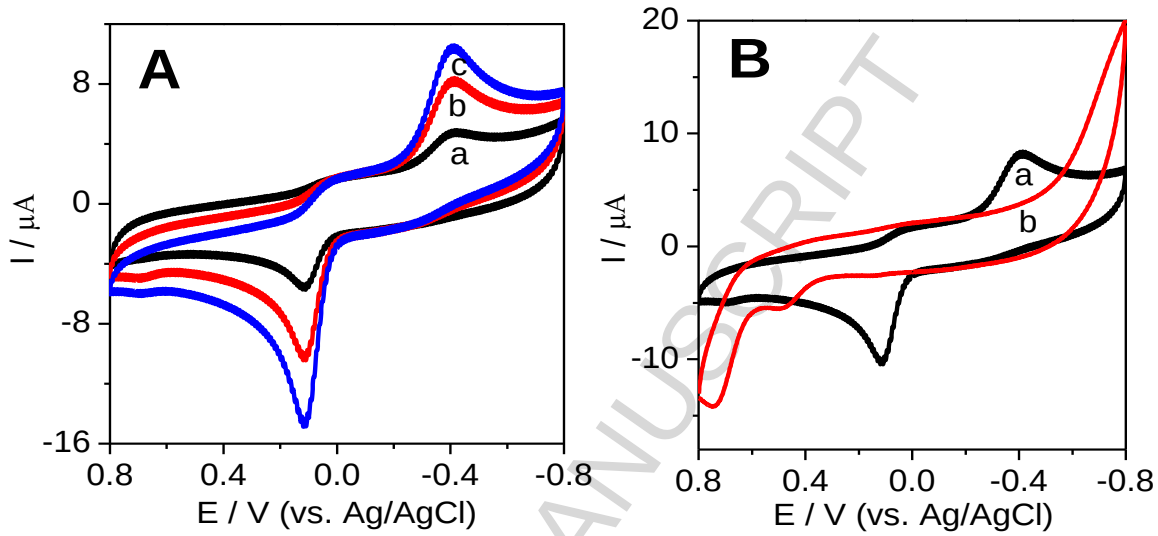

Fig. 4

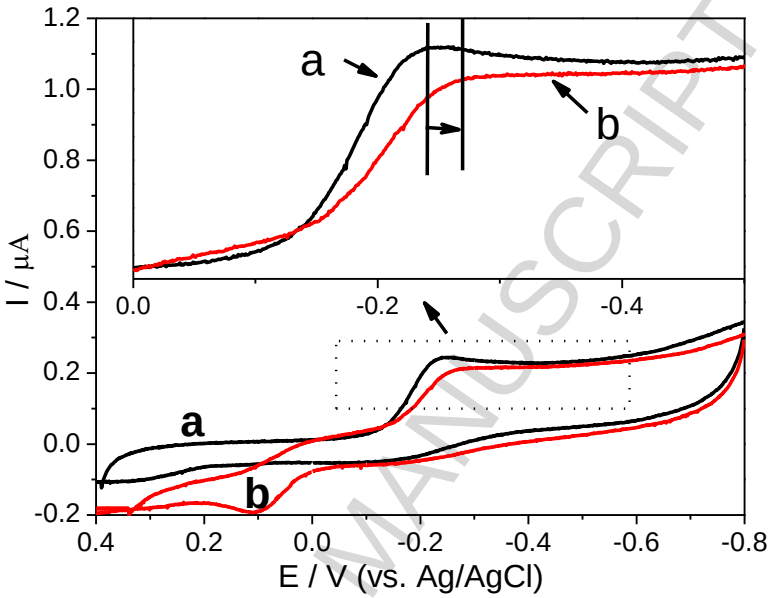

Fig. 5

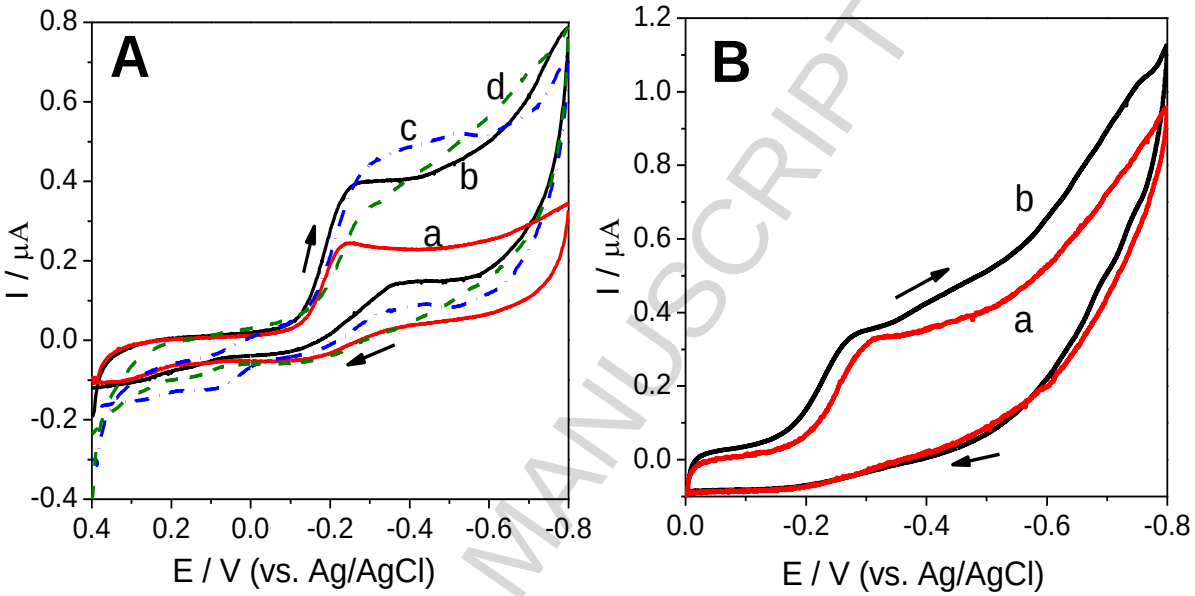

Highlights

►An electrochemically driven catalytic strategy was described ►Fast direct electron transfer between electrodes and D290nNOSoxy was observed ► D290nNOSoxy biocatalysis was successfully driven by electrodes in the presence of BH4 and oxygen